Chapter 8 3 September 2002 $M = 4.75$ Yorba Linda, California, earthquake

The $M = 4.75$ Yorba Linda, California earthquake occurred at $07:08:51.870$ UT on 3 September 2002 in Orange County, in a densely instrumented region of the seismic network. The mainshock was located by SCSN at $33.9173°N, -117.7758°W$ at a depth of 12.92 km. Two foreshocks, a $M = 2.66$ event at $2002/09/03, 04:50:48.330$ UT and a $M = 1.6$ event at $2002/09/03, 05:23:14.420$ UT, occurred within 1 km of the mainshock epicenter in the 24 hours prior to the mainshock. The faulting from the mainshock was primarily strike-slip on a vertical plane striking $N30°W$, consistent with the mainshock's proximity to the Whittier fault (Hauksson et al., 2002).

8.1 Road map

The Virtual Seismologist (VS) method for seismic early warning is applied to the Yorba Linda mainshock dataset, using seismograms from real-time telemetered SCSN stations. Following a few comments on the station geometry in the epicentral region, the VS single-station estimates for magnitude and epicentral distance based on the 3-second amplitudes at the first triggered station (SRN) are presented. Due to the high density of SCSN stations in the region, at the time of the first VS estimate (3 seconds after the initial P detection), there are enough arrivals at adjacent stations to uniquely determine the earthquake location.

The initial VS estimate is updated at 5, 8, 13, 38, and 78 seconds after the initial P detection (add 2 seconds to get VS estimate time relative to earthquake origin time). These updated VS estimates are expressed in terms of magnitude and epicentral location. There were 2 foreshocks within 1 km of the mainshock epicenter which occurred within the 24 hours preceding the mainshock. The foreshock information

is not as crucial as in other events considered (Hector Mine, San Simeon); due to the high station density, there are enough arrivals to uniquely constrain location 3 seconds after the initial P detection.

The first few VS estimates are the more important for seismic early warning. However, the VS estimates for large times after the earthquake origin or the initial P detection are also useful. They provide very robust amplitude-based locations (Kanamori, 1993), which can be used as checks on the more precise (but less robust) arrival-based locations. The amplitude-based location estimates for the Yorba Linda mainshock ground motions are discussed.

Finally, the observed peak P- and S-wave amplitudes are compared with the expected ground motion levels from the envelope attenuation relationships developed in Chapter 2. There is fairly good agreement between the predicted and observed ground motion amplitudes. This is expected, since the Yorba Linda ground motions were part of the dataset from which the envelope attenuation relationships were derived.

8.2 SCSN stations in the epicentral region

Figure 8.1 shows SCSN stations (triangles) within 200 km of the epicenter. The polygons are the Voronoi cells (nearest neighbor regions) of the various stations. An event is most likely to be located within the Voronoi cell of the station at which the first P wave trigger is detected (since the first triggered station is closest to the event). The SCSN station closest to the mainshock is Serrano (SRN), located at $33.83°N, -117.79°W$, at an epicentral distance of 9.9 km. SRN's nearest neighbor region (Voronoi cell) is shaded in Figure 8.1. This region has an area about $436 km^2$. The largest epicentral distance within SRN's Voronoi cell is 14.8 km. The mainshock, as well as the two foreshocks, are located within SRN's Voronoi cell. Table 8.1 lists the stations immediately surrounding SRN (and thus sharing a Voronoi edge with SRN).

Figure 8.2 shows the observed vertical acceleration records from SRN, the first

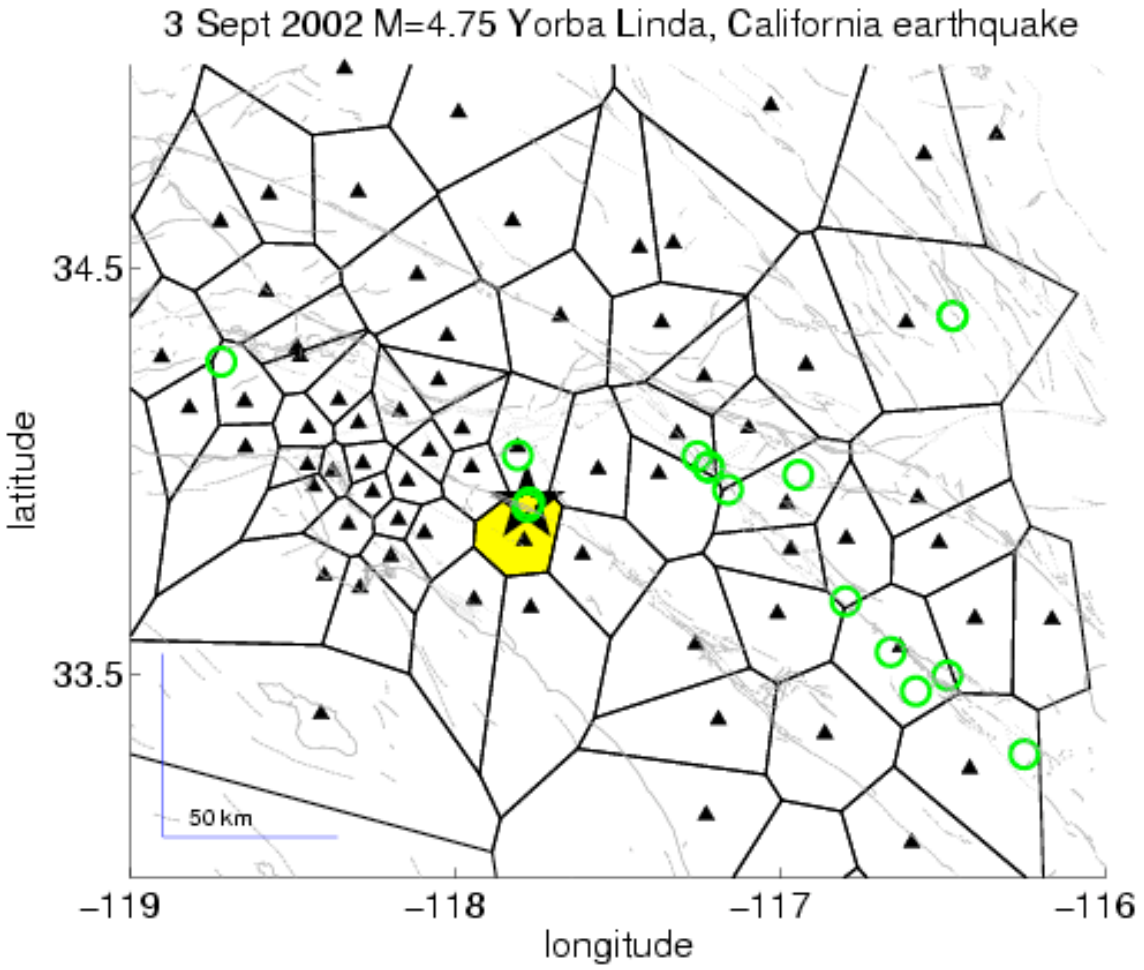

Figure 8.1: Map showing SCSN stations (and their Voronoi cells) within 200 km of the $M = 4.75$ Yorba Linda, California mainshock. Circles are locations of $M \geq 1$ earthquakes reported by the network in the 24 hours prior to the mainshock. Two foreshocks occurred within the Voronoi cell of SRN (shaded), the SCSN closest to the mainshock epicenter.

Stations closest to the $M = 4.75$ Yorba Linda mainshock

Station name	Abrev	Lon	Lat	vor. area km^2	ep. dist. km	Arrv. sec
Serrano	SRN	-117.789	33.829	436	9.9	2.2 (0)
CalPoly Pomona	CPP	-117.809	34.060	556	17.1	3.1 (0.9)
Walnut	WLT	-117.951	34.009	269	19.1	3.65 (1.45)
Pleasants Peak	PLS	-117.609	33.795	710	20.5	3.95 (1.75)
Mira Loma Subst.	MLS	-117.561	34.005	612	22.1	4.05 (1.85)
Santiago	STG	-117.769	33.664	1591	28.1	4.9 (2.7)
Ellis	LLS	-117.943	33.684	1027	30.1	5.9 (3.7)
Del Amo	DLA	-118.096	33.848	284	30.6	6.05 (3.85)

Table 8.1: Some SCSN stations within 30 km of the $M = 4.75$ Yorba Linda mainshock. The SCSN station closest to the mainshock is Serrano (SRN) at an epicentral distance of 9.9 km. The other stations listed share a Voronoi edge with SRN. In the rightmost column, the first number is time of the P wave arrival, in seconds after the earthquake origin time. However, the origin time is unknown and must be solved for. What is observed is the time interval between the P arrival at a given station and the first detected P arrival (in parentheses). In this example, the first detected P wave is at SRN. For the other stations, the value in parentheses is the interval in seconds between the P arrival at that given station and the P arrival at SRN.

triggered station, and the adjacent stations sharing a Voronoi edge with SRN. Due to the high density of SCSN stations in the epicentral region, at the time of the initial VS estimate 3 seconds after the initial P detection, there are enough P arrivals to uniquely determine the epicentral location.

8.3 Single station estimates: solving for magnitude and epicentral distance

With data from only a single station, the VS method can be used to solve for magnitude and epicentral distance, or magnitude and location coordinates. The VS estimates for magnitude and epicentral distance using the first 3 seconds of data from SRN are presented first.

Let Z.a, Z.v, and Z.d refer to the maximum vertical acceleration, velocity, and filtered displacement envelope amplitudes observed between the P detection at a station and some time t. (In the examples in this thesis, it is assumed that P-waves can be detected efficiently using short-term over long-term average methods.) EN.a, EN.v, and EN.d are the corresponding envelope amplitudes for the root mean square of the maximum amplitudes of the horizontal channels.

Figure 8.3 (a) shows the shows the P/S discriminant function (discussed in Appendix C) as a function of time. The P/S discriminant function is $PS = 0.4\log_{10}(Z.a) + 0.55\log_{10}(Z.v) - 0.46\log_{10}(EN.a) - 0.55\log_{10}(EN.v)$. The first zero crossing of P/S after the P arrival indicates the S-wave arrival. The method expects the P-wave to be larger on the vertical and smaller on the horizontal, and the converse for the S-wave. As discussed in Appendix C, this discriminant has a misclassification error of 15%. There is fairly good agreement between the actual S-wave arrival and the estimated arrival using the P/S discriminant. Figure 8.3(b) shows ratio $Z_{ad} = Z.a^{0.36}/Z.d^{0.93} = 0.36\log_{10}(Z.a) - 0.93\log_{10}(Z.d)$ as a function of time. The left-hand axis shows the P-wave decision boundaries; those on the right, the S-wave decision boundaries. The peak vertical ground motions at SRN indicate that the

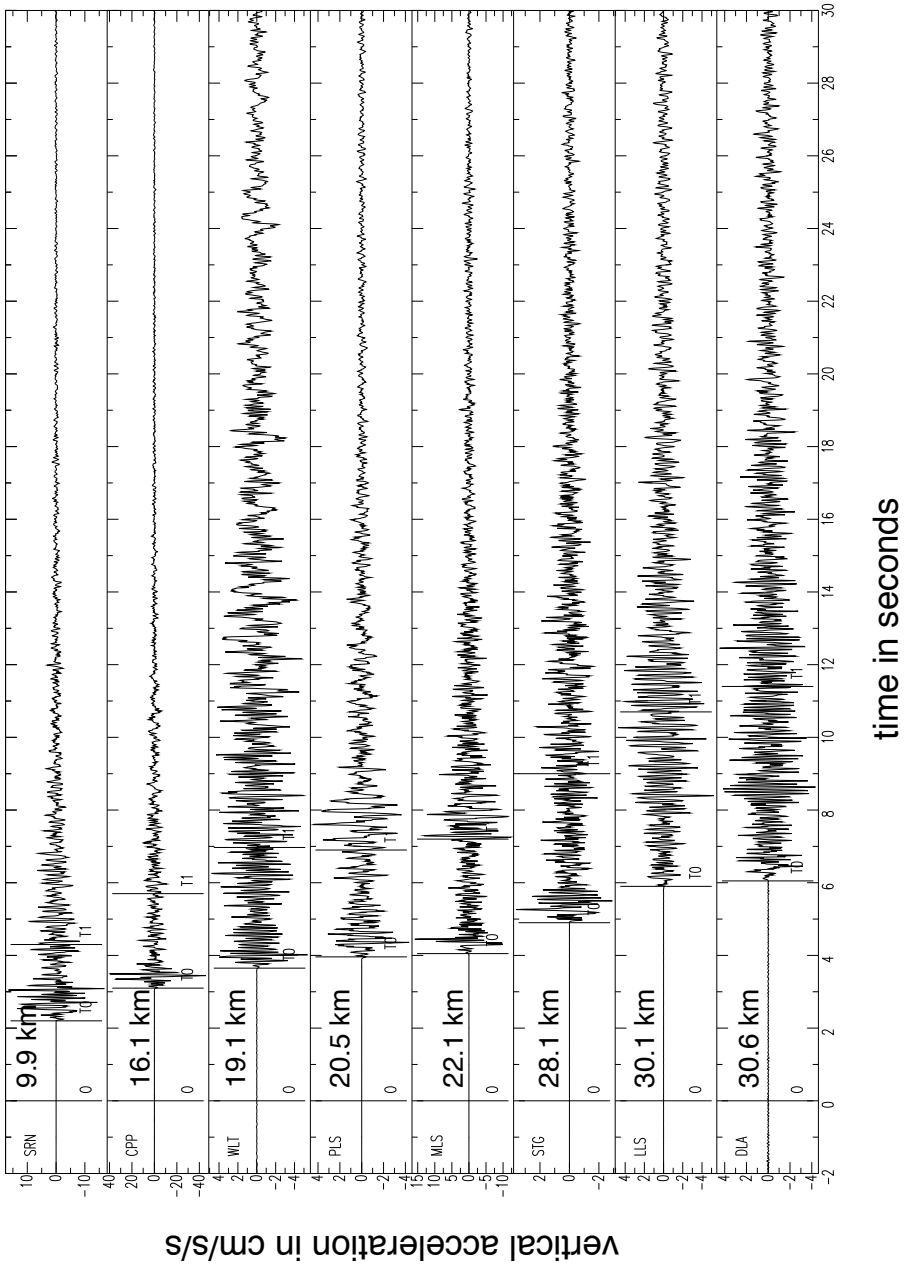

Figure 8.2: Vertical acceleration records from stations within 30 km of the Yorba Linda mainshock. Vertical lines marked "t_0" and "t_1" are the P and S arrival times, respectively. Arrival times were calculated using Eaton's travel time code with a 1D, 6 layer Southern California velocity model and adjusted manually if there were large discrepancies between the calculated and observed arrivals. The earthquake origin time is t=0 in this plot.

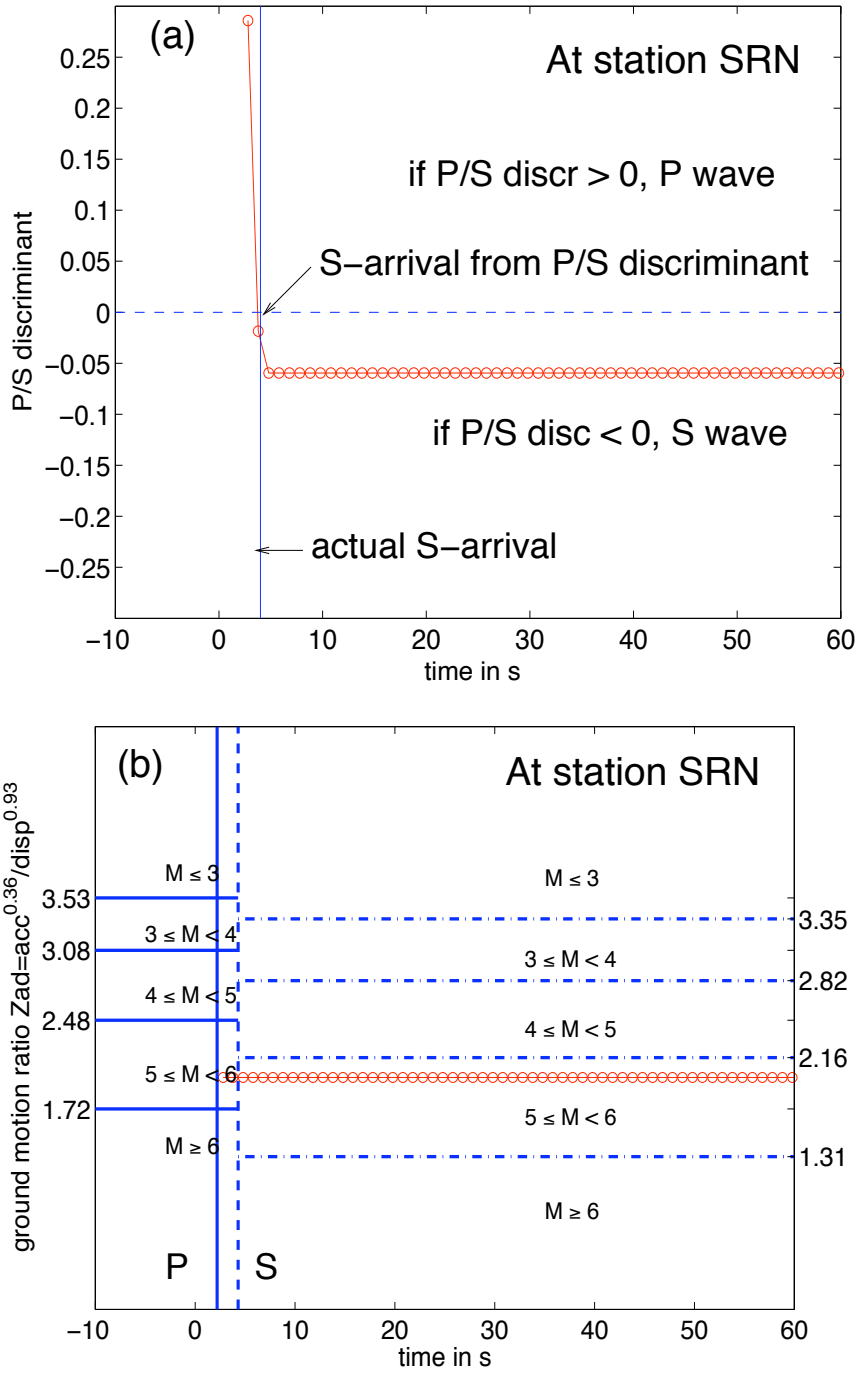

Figure 8.3: (a) The P/S discriminant $Z_{PS} = 0.43\log_{10}(Z.a) + 0.55\log_{10}(Z.d) - 0.46\log_{10}(EN.a) - 0.55\log_{10}(EN.d)$ at SRN as a function of time. If $Z_{PS} > 0$, the amplitudes are most likely from a P wave. If $Z_{PS} < 0$, they are most likely from an S-wave. The estimated S arrival is in agreement with the observed S arrival. (b) The ground motion ratio, $Z_{ad} = \frac{acc^{0.36}}{disp^{0.93}}$ at SRN as a function of time. The P-wave decision boundaries are shown on the left hand axis, the S-wave decision boundaries are shown on the right. The ground motion ratios indicate that the event is $5 \leq M \leq 6$.

event is between $5 \leq M \leq 6$. From Chapter 4 (Table 4.4), if, based on the observed P-wave ground motion ratios, an event is classified as $5 \leq M \leq 6$ (or Group 4), this is the correct classification 80% of the time; there is a 15% chance that the event is actually from the lower magnitude group $4 \leq M \leq 5$, and a 6% chance that the event is actually from the larger magnitude group $M \geq 6$.

The likelihood function described in Chapter 4 combines the magnitude estimates from the vertical acceleration and displacement ground motion ratio, along with the peak available vertical velocity, and rms horizontal acceleration, velocity, and displacement amplitudes to estimate magnitude and epicentral distance. Maximizing the likelihood function yields the source estimates (in this case, magnitude M and epicentral distance R_{SRN}) that are most consistent with the available observations. Figure 8.4 shows contours of the likelihood function expressed in terms of M and R. The likelihood is scaled to have a maximum value of 1; contours are drawn at the 0.6, 0.1, and 0.01 levels, which correspond to $\pm 1\sigma$, $\pm 2\sigma$, and $\pm 3\sigma$ about the mean of a 1-d Gaussian pdf. The "high" probability region within the 0.6 level contour is shaded; the actual magnitude and epicentral distance (star) is included in this region. Trade-offs between M and R cannot be resolved by the 3 second observations; this is evident from the elongated contours of the likelihood function. In the absence of additional data, such trade-offs can be resolved by introducing prior information into the estimation process. While trade-offs do exist, the likelihood function does have a peak. An M=5.5 event located 33 km away from SRN is the source estimate most consistent with the envelope attenuation relationships and the available peak amplitudes 3 seconds after the initial P detection at SRN. (The Yorba Linda mainshock had magnitude M=4.75 and an epicenter located 9.8 km away from SRN.)

When expressing the problem in terms of magnitude and epicentral distance, the only prior information that can be included are 1) the range of epicentral distances consistent with the Voronoi cell of the first triggered station and 2) the Gutenberg-Richter magnitude-frequency relationship. The first P wave detection is at SRN and the geometry of operating stations defines nearest neighbor regions, which in turn provides constraints on earthquake location given the first P detection. If all locations

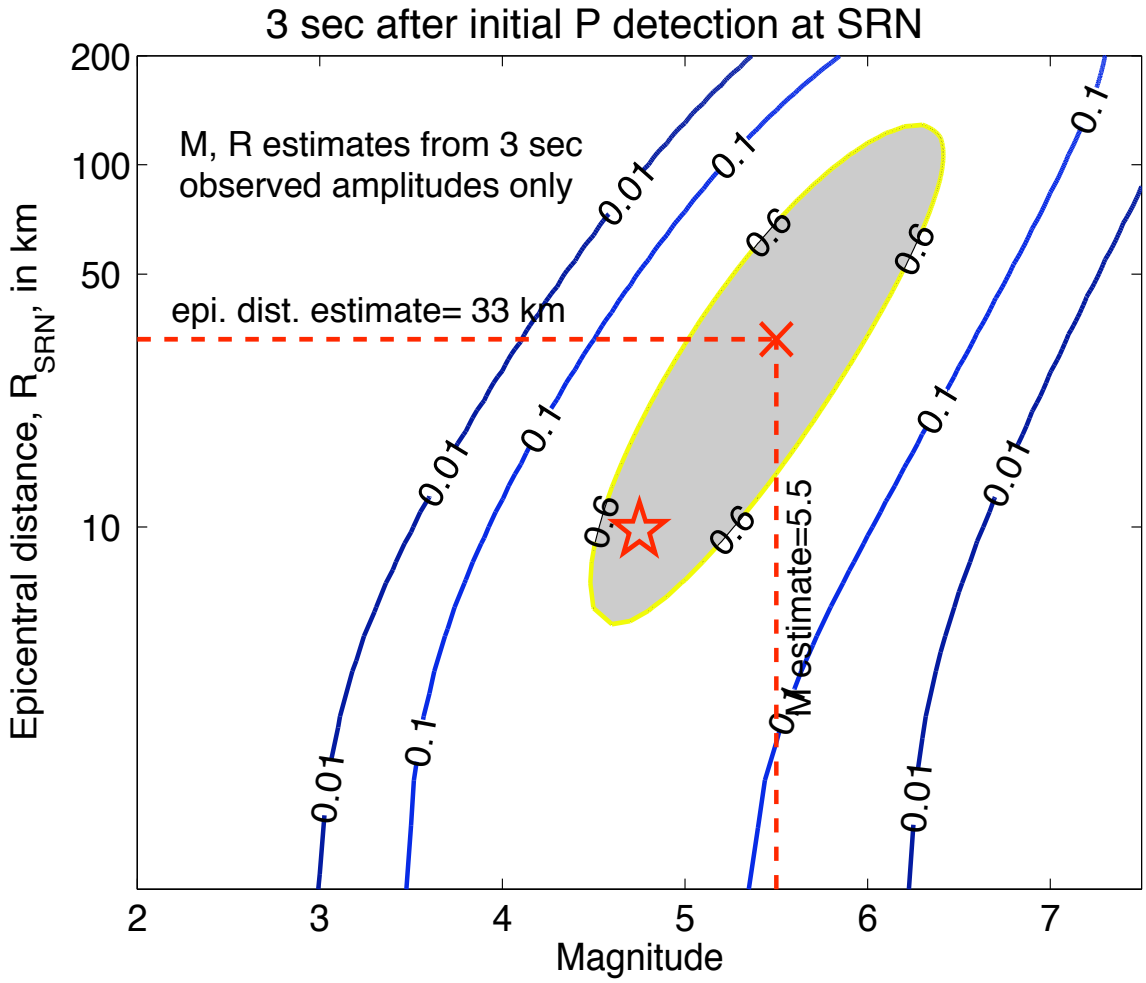

Figure 8.4: Contours of the likelihood function (expressed in terms of magnitude and epicentral distance) given the amplitudes at SRN 3 seconds after the initial P detection. Contours are drawn at 0.6, 0.1, 0.01 levels. Regions where the likelihood function has value > 0.6 are shaded. The star marks the actual magnitude (M=4.75) and epicentral distance (9.8 km) of the Yorba Linda mainshock.

within SRN's Voronoi cell are given equal weight, certain epicentral distances will have more weight. A probability density function for epicentral distances consistent with being within SRN's Voronoi cell (and thus consistent with a first P detection at SRN) can be constructed. This is shown in Figure 8.5. The maximum possible epicentral distance consistent with an initial P detection at SRN is 15 km. Figure 8.6 shows contours of the Bayes posterior density function, whose maxima correspond to the VS estimates, with (a) and without (b) the Gutenberg-Richter magnitude-frequency relationship in the Bayes prior. In both Figures 8.6(a) and (b), the epicentral distance constraint from station geometry is used. The Gutenberg-Richter (G-R) relationship states that smaller earthquakes occur more frequently than larger events. Using the G-R relationship in the prior resolves trade-offs in favor of smaller magnitude events at closer distances to the station. With the G-R in the prior, the VS estimate is an $M = 4.4 \pm 0.39$ event located 8 km from SRN. Without the G-R, the VS estimate is an $M = 4.8 \pm 0.43$ event located 9 km from SRN. SCSN reported the Yorba Linda mainshock as an M=4.75 event; based on the SCSN location, the epicenter was 9.8 km away from SRN.

8.4 Multiple station estimates: solving for magnitude and epicentral location

The relatively high density of SCSN station within the epicentral region mean that the inter-station distance is low; at the time of the initial VS estimate 3 seconds after the P detection at SRN, there are enough arrivals at the adjacent stations to uniquely determine the epicentral location. The inclusion of observations from multiple stations is most conveniently addressed using a geographic coordinate system, or by expressing the likelihood function in terms of magnitude and epicentral location, as opposed to epicentral distance. This change in coordinate system also allows information about fault locations and previously observed seismicity to be included in the Bayes prior. There were two foreshocks within 1 km of the mainshock epicenter in the 24 hours

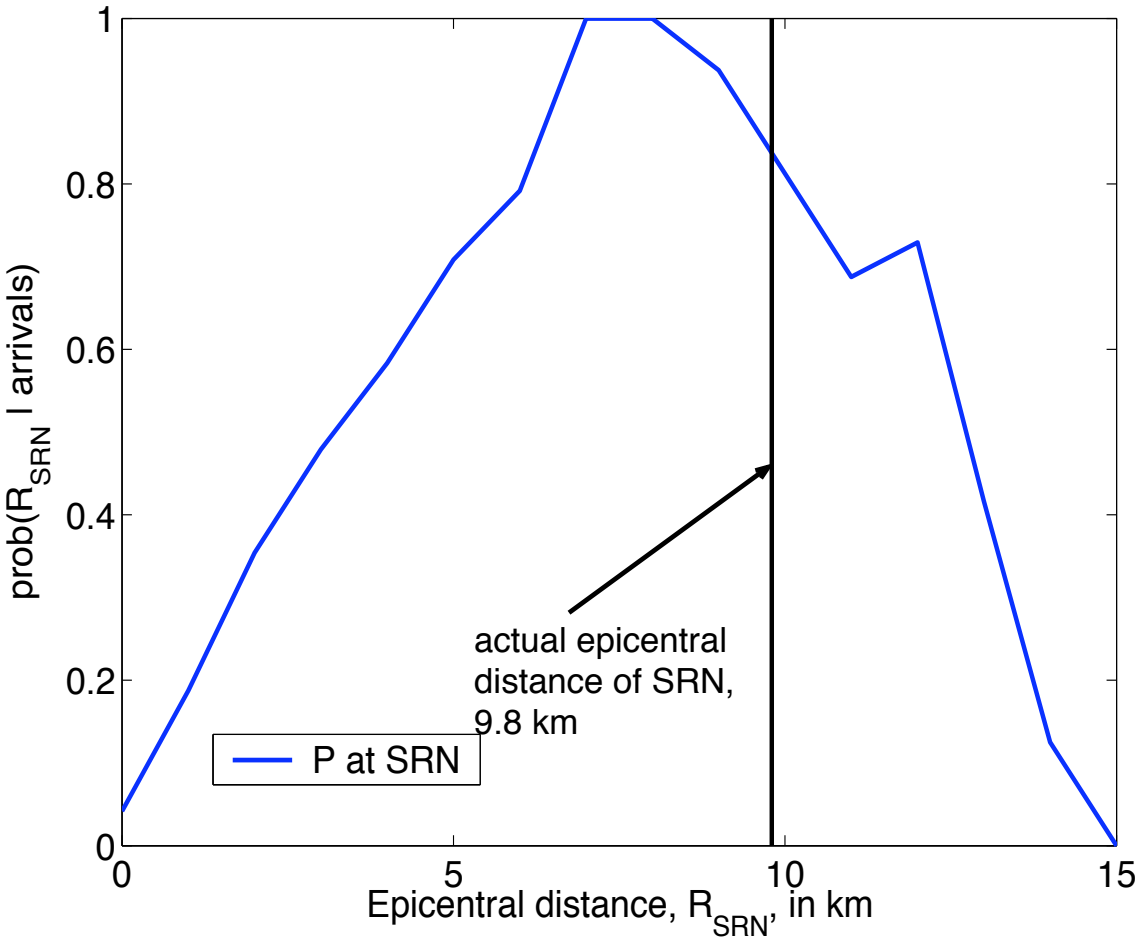

Figure 8.5: The range of possible epicentral distances, R_{SRN}, consistent with a first P detection at SRN. The weights on various distances (y axis) are obtained by giving equal weight to all locations within SRN's Voronoi cell.

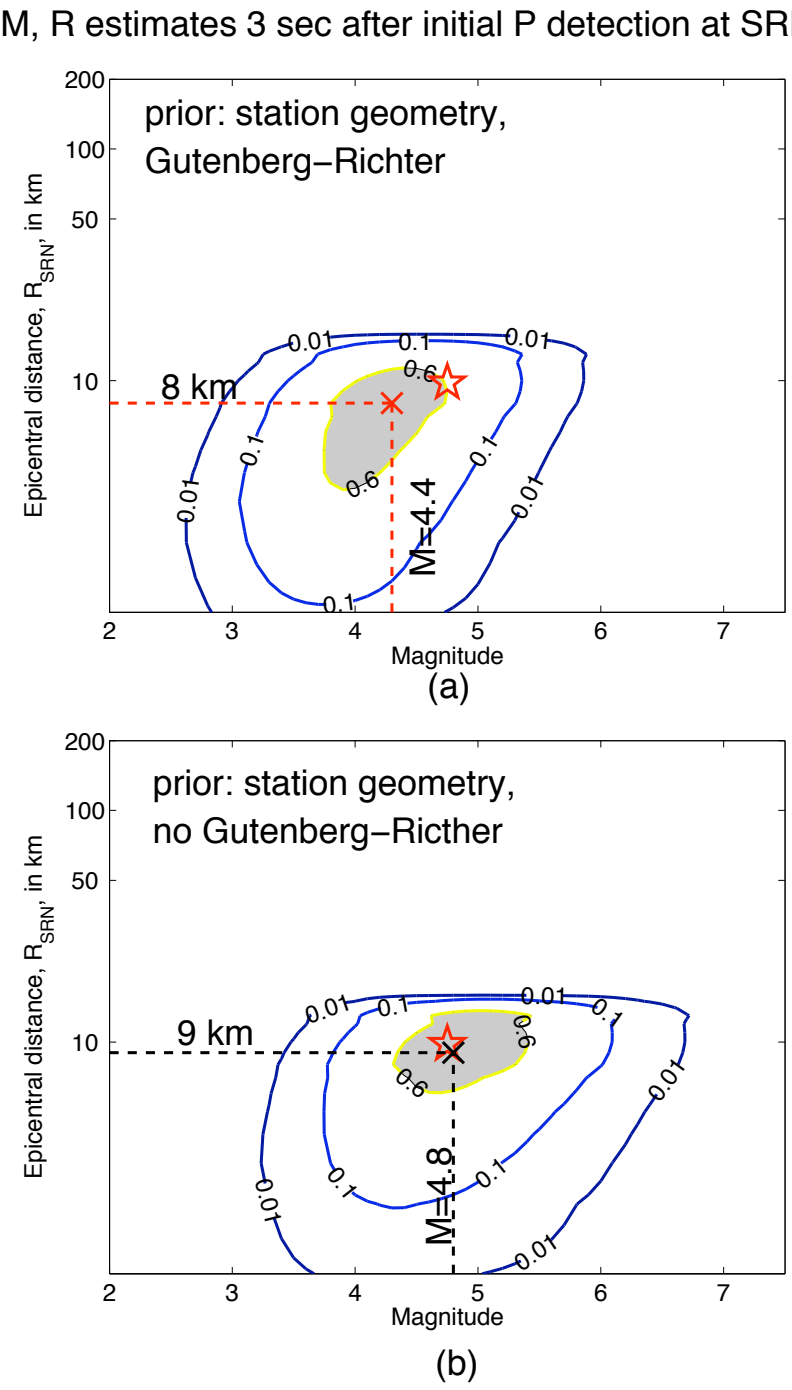

Figure 8.6: Whether or not the Gutenberg-Richter magnitude-frequency relationship is included in the Bayes prior affects the shape of the Bayes posterior, and hence the VS estimates, given the peak amplitudes at SRN 3 seconds after the P detection. Regions in M-R space where the Bayes posterior density function, $prob(M, R|data) \geq 0.6$ are shaded. The star marks the actual magnitude and epicentral distance of the Yorba Linda mainshock. The Gutenberg-Richter relationship favors smaller magnitude events located at closer distances to the station.

preceding the mainshock. This information is included in the Bayes prior; fault information is not included. The Bayes prior is not as important for the Yorba Linda event as it was for the Hector Mine, San Simeon, and Parkfield earthquakes. At the time of the initial VS estimate 3 seconds after the P detection at SRN, the P waves have propagated to at least 2 more adjacent stations, and the epicentral location is uniquely determined.

Figure 8.7 shows contours of the P-wave wavefront at the times of various VS estimates- at 3, 5, 8, 13, 38, and 78 seconds after the initial P detection (add 2.2 to get VS estimate times relative to earthquake origin time).

From Figure 8.7, by the time of the initial VS estimate 3 seconds after the first P detection, the P waves have already arrived at a total of 7 stations. Thus, the epicentral location is uniquely determined by the P-wave arrivals. Just the same, seismicity and station geometry priors are generated in a similar manner as they were for the other examples. The seismicity prior is generated by assigning locations within a 5 km radius of an earthquake in the preceding 24 hours a particular weight. This weight was chosen to be 5 for this event; the combined effect of the two foreshocks within SRN's Voronoi cell weights their locations 25 times more than other locations. A scaling factor is introduced such that the seismicity prior integrates to 1 over the latitude and longitude range considered. For simplicity, the seismicity prior is independent of magnitude. There are formal ways to quantify how previously observed seismic activity affects earthquake probabilities. In practice, foreshock/aftershock statistics such as those described by Reasenberg and Jones (1989) and Gerstenberger et al. (2003) should be used to generate the seismicity prior.

The station geometry prior is generated by calculating the nearest neighbor regions of the operating stations. Locations within the first triggered station's Voronoi cell are assigned a weight of 100; all other locations are assigned a weight of 1. A scaling factor is introduced such that the station geometry prior integrates to 1 over the latitude and longitude range considered. The location prior $prob(lat, lon)$ is obtained by multiplying the seismicity and station geometry priors.

The various updates to the VS estimates are calculated with and without the

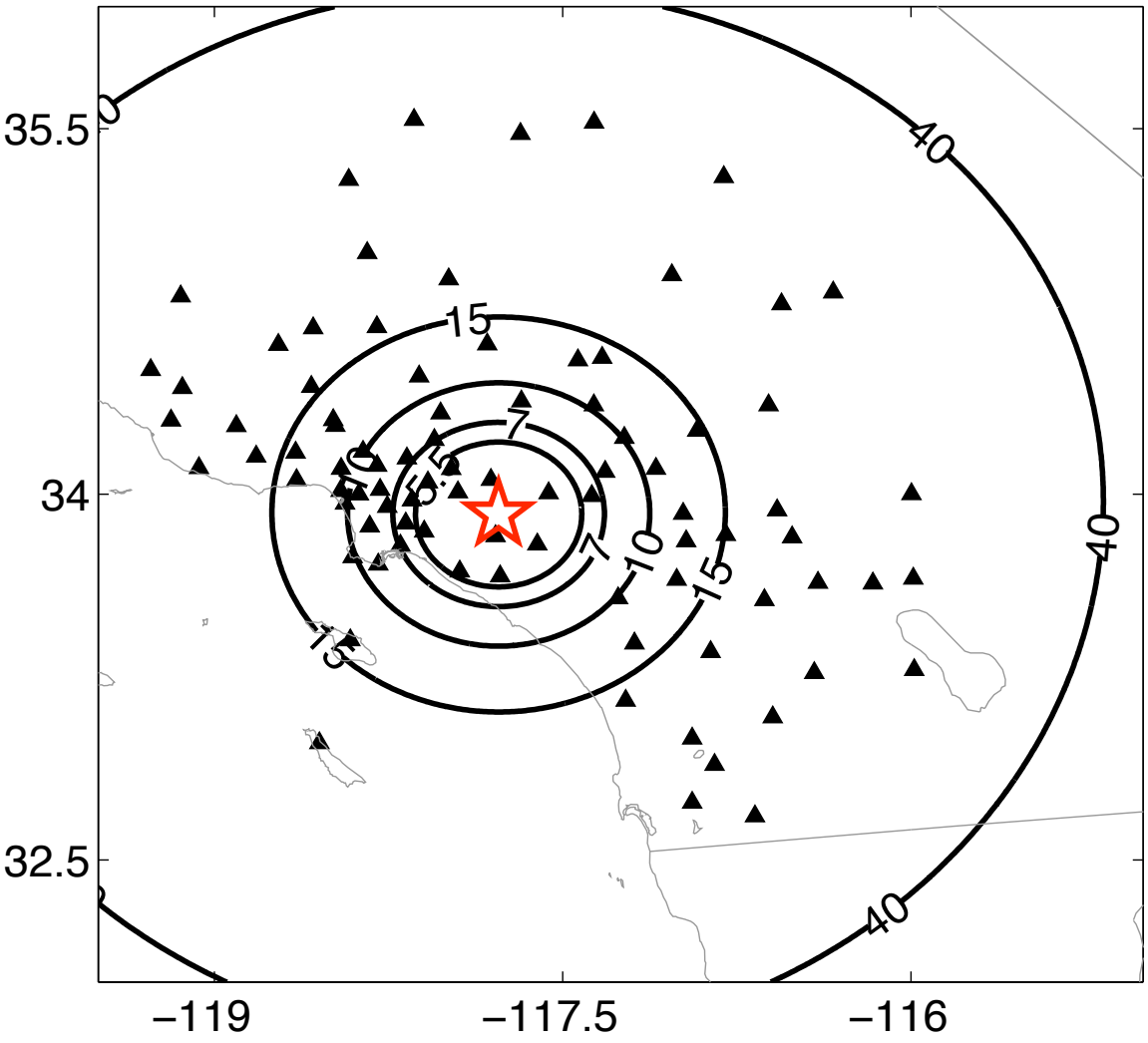

Figure 8.7: SCSN stations used to update the VS estimates for the 2002 M=4.75 Yorba Linda mainshock. Contours show the P-wave wavefront (for a point source at the epicenter) at the times of the VS estimates at t=3, 5, 8, 13, 38, and 78 seconds after the initial P detection (add 2.2 to get VS estimate times relative to earthquake origin time). The labels on the Figure are for VS estimate times relative to the origin time. The 80 second contour is beyond the boundaries of the plot.

Gutenberg-Richter relationship. When the Gutenberg-Richter relationship is used, the magnitude prior has the form $prob(M) = 10^{1-M}$; when it is not included, the magnitude prior is $prob(M) = k$, where k is a constant. The magnitude prior is scaled so that it integrates to 1 over the magnitude range considered ($2 \leq M \leq 7.5$). The Bayes prior is the product of the magnitude and location priors. That is, $prob(M, lat, lon) = prob(M) \times prob(lat, lon)$. Again, it is a simplifying assumption to treat the magnitude and location information as independent.

Given only the peak amplitudes at SRN 3 seconds after the initial P detection (no arrival information other than the first P detection at SRN, no prior information), Figure 8.8 shows the locations consistent with 6 different magnitude ranges: $2 \leq M < 3$, $3 \leq M < 4$, $4 \leq M < 5$, $5 \leq M < 6$, $6 \leq M < 7$, and $M \geq 7$. For each magnitude range, the contours of the location marginal of the likelihood function (integrated over the given magnitude range and scaled to a maximum value of 1) are drawn at the 0.01, 0.1, and 0.6 levels. The regions where $prob(lat, lon|data) \geq 0.6$ are shaded.

The VS estimate for magnitude and epicentral location 3 seconds after the initial P detection is a combination of the Bayes prior, the likelihood function given the available amplitudes (Figure 8.8), as well as constraints on earthquake location given the available P arrivals. Due to the high density of SCSN stations in the epicentral region, there are enough arrivals available at the time of the initial VS estimate to uniquely locate the epicenter. Figure 8.9 illustrates the hyperbolic location method described by Rydelek and Pujol (2004) with the P arrivals available 3 seconds after the initial P detection at SRN. In Figure 8.10, the color scales with the probability of the event being located at a given location; the contours convey the magnitude estimate without the Gutenberg-Richter magnitude-frequency relationship. The VS location estimate is within 0.89 km of the SCSN-reported epicenter. The VS magnitude estimate *without* G-R is $M = 4.8 \pm 0.425$; *with* G-R, it is $M = 4.4 \pm 0.39$. (The actual magnitude, as reported by SCSN, is M=4.75.) While the VS location estimates will not change much with additional observations, the magnitude estimates continue to evolve.

Figure 8.11 shows the availability of arrival and amplitude observations as a func-

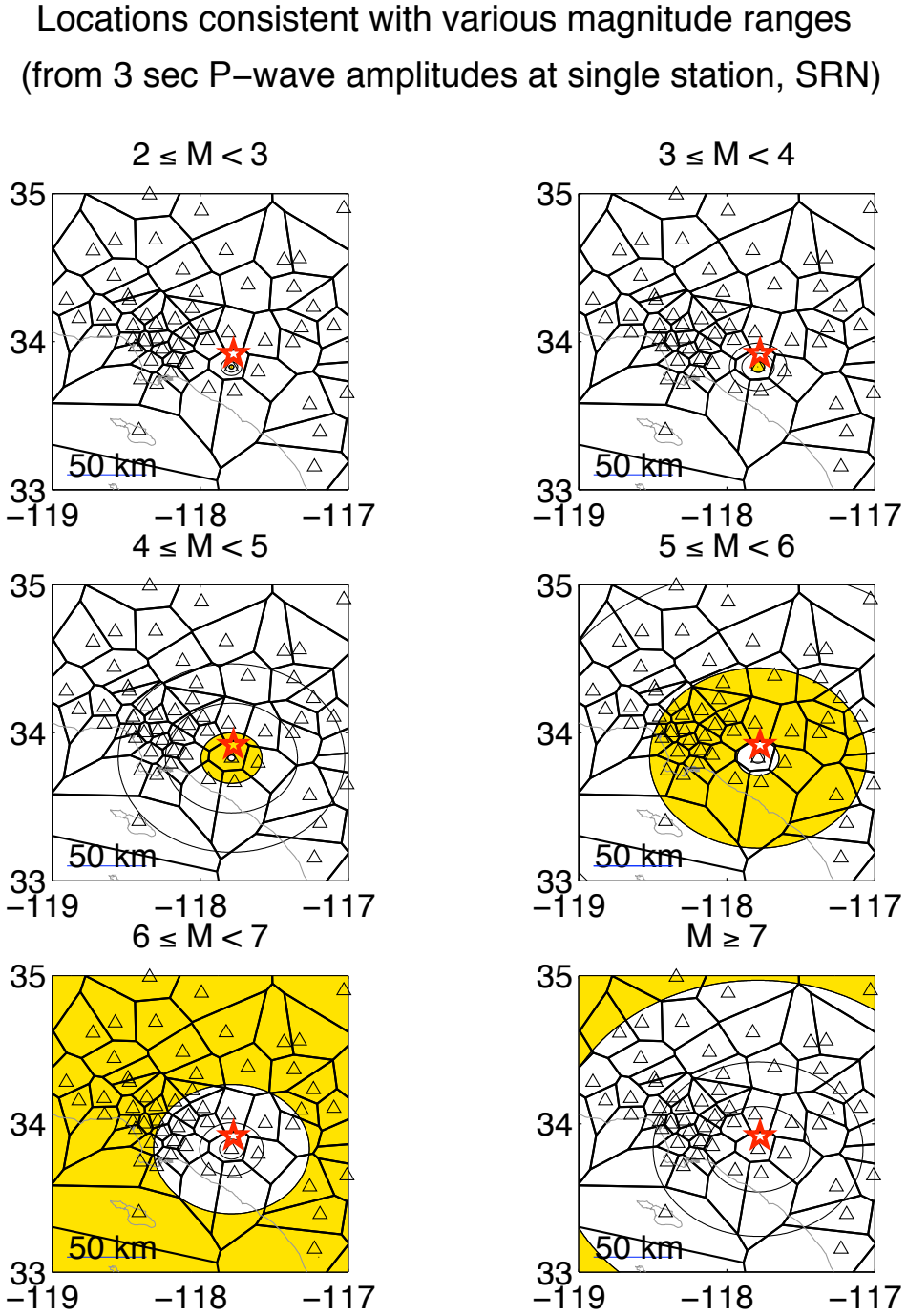

Figure 8.8: The shaded regions in each subplot are the locations consistent with the given magnitude range using the peak P-wave amplitudes 3 seconds after the initial P detection at SRN (not accounting for arrivals at surrounding stations or prior information). 3 seconds of P-wave amplitudes from the first triggered station cannot uniquely resolve magnitude and location (although this information is enough to broadly estimate the probable magnitude range). The trade-offs shown here are comparable to those shown in Figure 8.4.

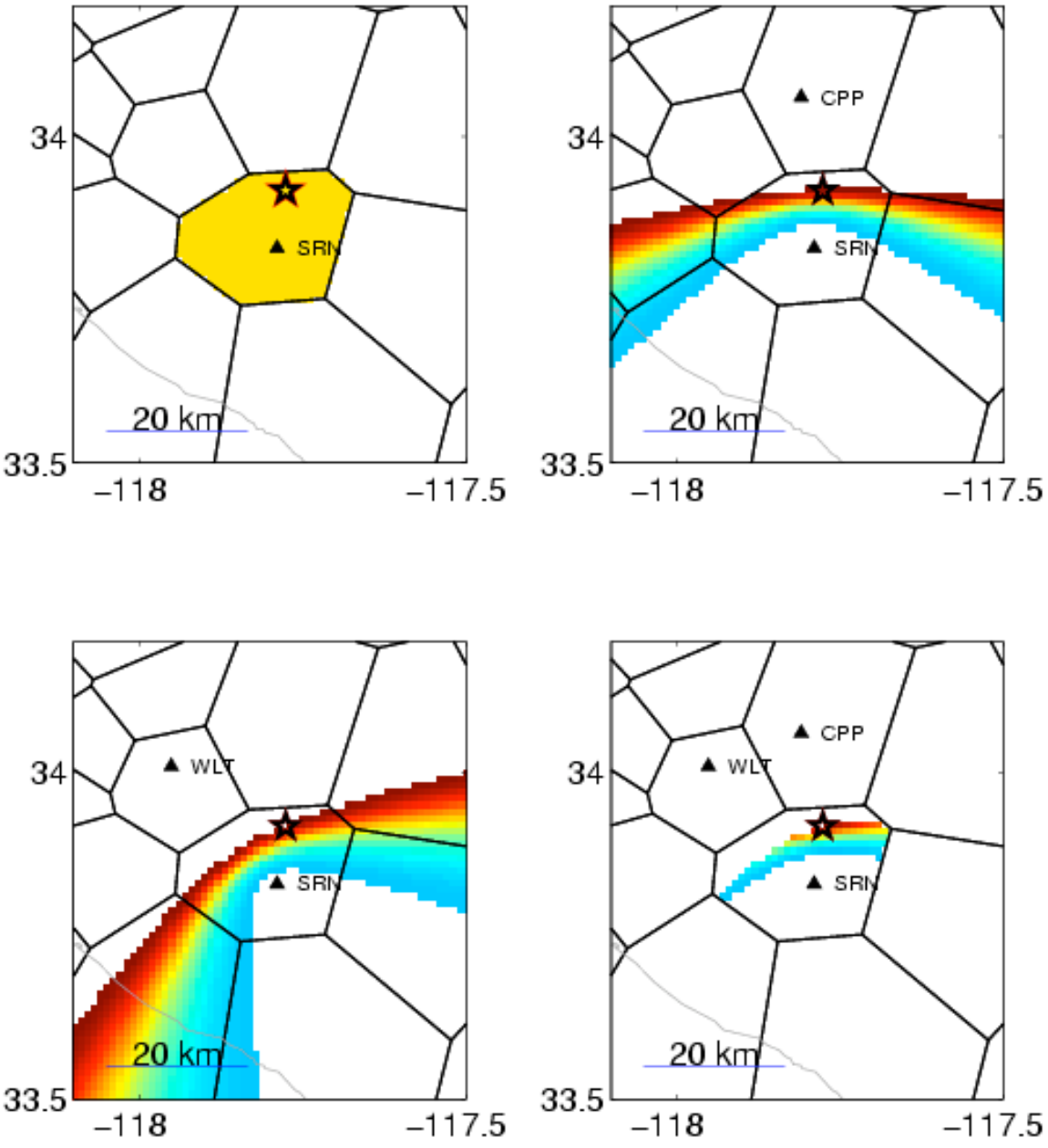

Figure 8.9: The colored regions are those consistent with (a) the first P detection at SRN, (b) a P detection at CPP 1 second after the P detection at SRN, (c) a P detection at WLT 1 second after the P detection at SRN, and (d) the combined sequence of P arrivals. At the time of the VS estimate 3 seconds after the initial P detection, there is enough arrival information to uniquely constrain the epicentral location.

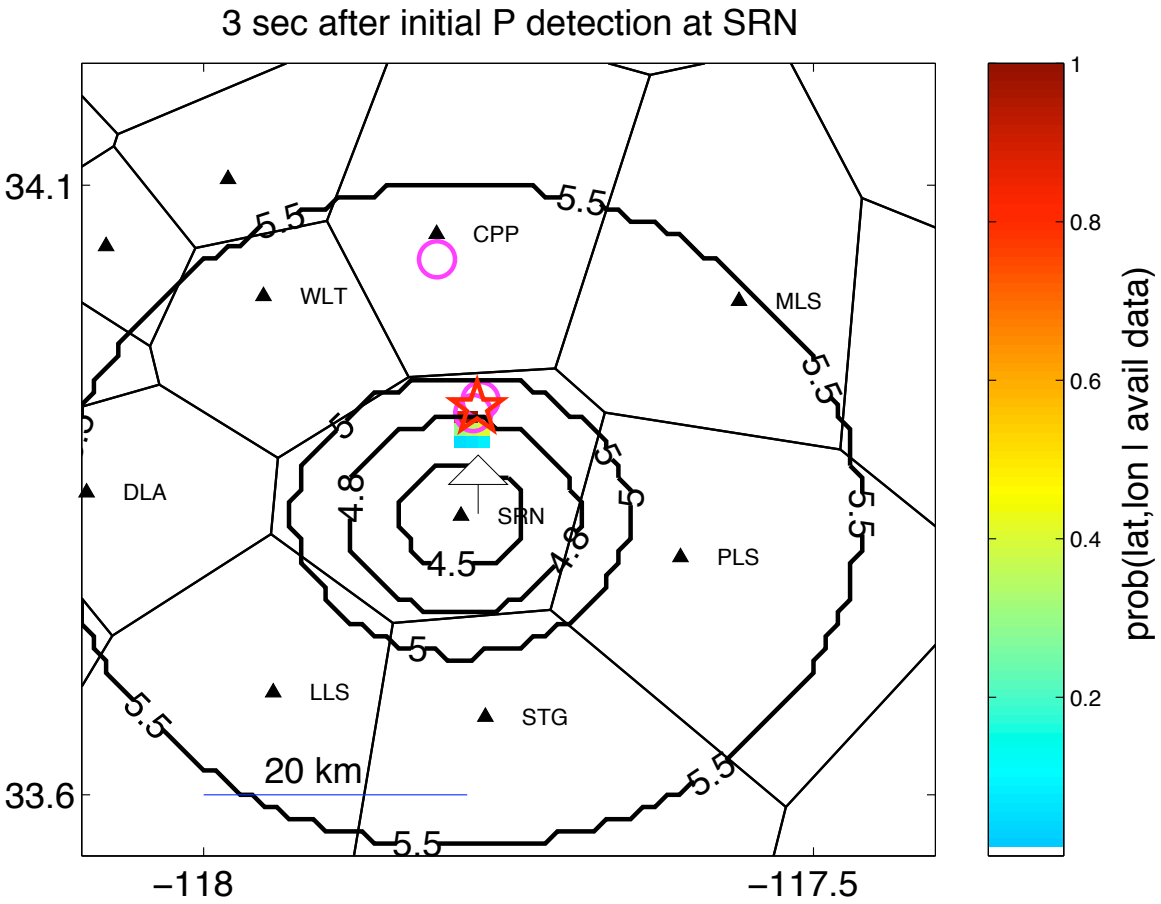

Figure 8.10: The colors scale with the probability that the earthquake is at a given location. There are enough P arrivals to uniquely locate the epicenter (arrow). A star marks the SCSN-reported epicenter. The circles are the previously observed seismicity in the preceding 24 hours. The contours convey the VS magnitude estimates without G-R, based on the peak amplitudes available 3 seconds after the initial P detection at SRN. The VS magnitude estimate *without* G-R is $M = 4.8 \pm 0.425$; *with* G-R, it is $M = 4.4 \pm 0.39$. The SCSN-reported magnitude is M=4.75.

tion of time. For seismic early warning, the earlier estimates are the most important. The Yorba Linda mainshock is not typical in that there is enough information within 3 seconds to uniquely determine the epicentral location. As illustrated by the other earthquakes examined in this thesis, it is more typical to have the an initially under-determined estimation problem. It is in this situation that the prior information is useful. Prior information is just a way to resolve trade-offs in parameters when the problem is under-determined; it is (and should be) irrelevant when there are enough available observations. The amount of time after the initial P detection necessary for the estimation process to go from under-determined to having a unique solution (at least for the epicentral location) depends on the station density in the epicentral region. Thus, prior information is most useful for regions where there is low station density.

Figure 8.12 shows the distance between the VS location estimate and the actual (SCSN) epicenter as a function of time. The VS location estimates are always within 4 km of the actual SCSN-reported epicenter. The VS location estimates are obtained via the hyperbolic method described by Rydelek and Pujol (2004) for the stations sharing a Voronoi edge with SRN, the first triggered station. The initial VS magnitude estimate (without G-R) is $M = 4.8 \pm 0.425$, within 0.05 magnitude units of the actual magnitude. The evolution of the VS magnitude estimates with time is shown in Figure 8.13. The error bars on the magnitude estimates decrease as $1/\sqrt{N}$, where N is the number of stations contributing observations to the VS estimate.

The VS estimates at 80 seconds after the origin time (or 78 seconds after the initial P detection) are not useful for seismic early warning; if this were a damaging event, the large ground motions would have, by this time, propagated to the areas that would have had strong shaking. However, the VS estimates (using a uniform prior) at large times after the origin or initial P detection provide very robust amplitude-based location estimates. Figure 8.14 shows the SCSN-reported location (star), the arrival-based location contours (blue), and the amplitude-based location contours(green). The arrival-based location (blue contours) are obtained by minimizing the residual between the predicted and 89 observed arrival times available 78 seconds after the

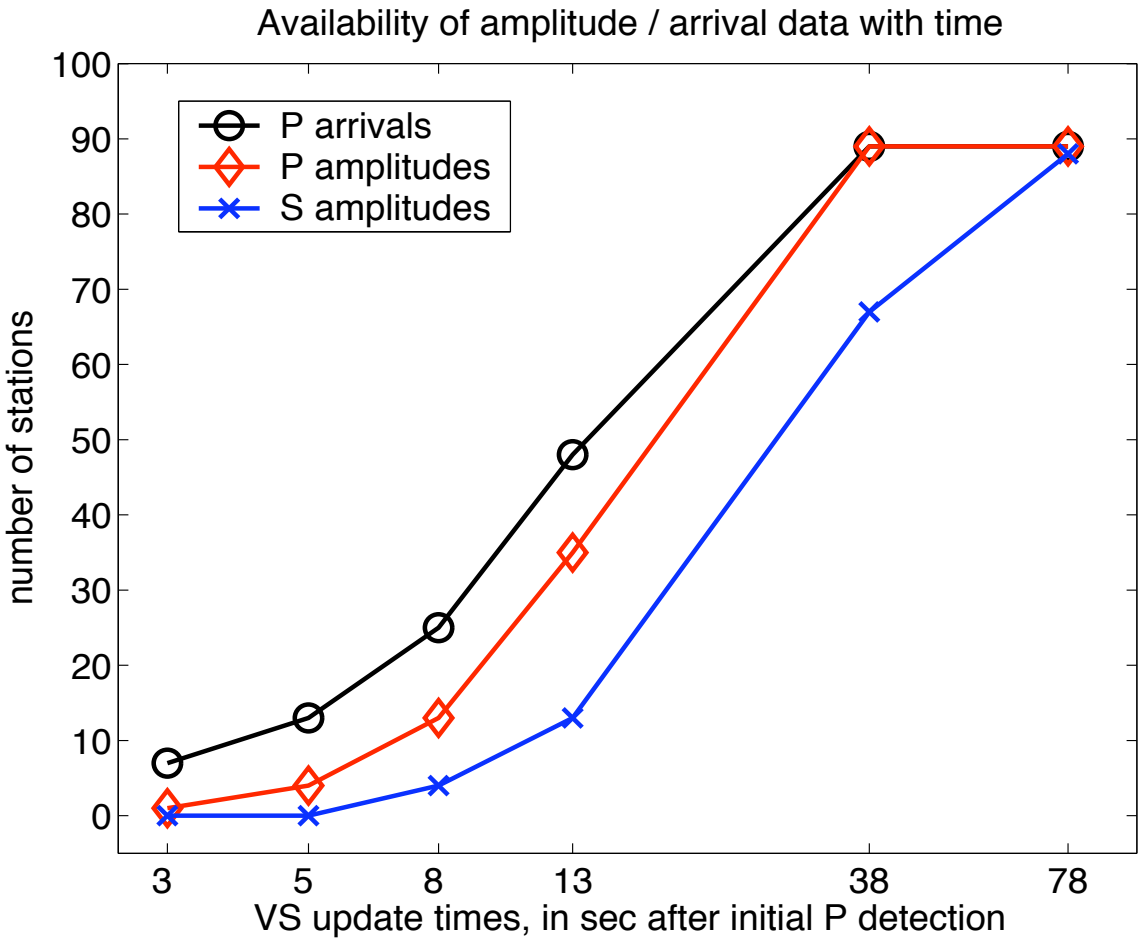

Figure 8.11: The number of stations contributing P-wave arrivals and peak P and S wave amplitudes to the VS estimates as a function of time. The seismicity and station geometry priors are not crucial to the VS location estimates; due to the high density of SCSN stations in the epicentral region, the epicenter is uniquely determined by observed P arrivals at the time of the initial VS estimate 3 seconds after the initial P detection.

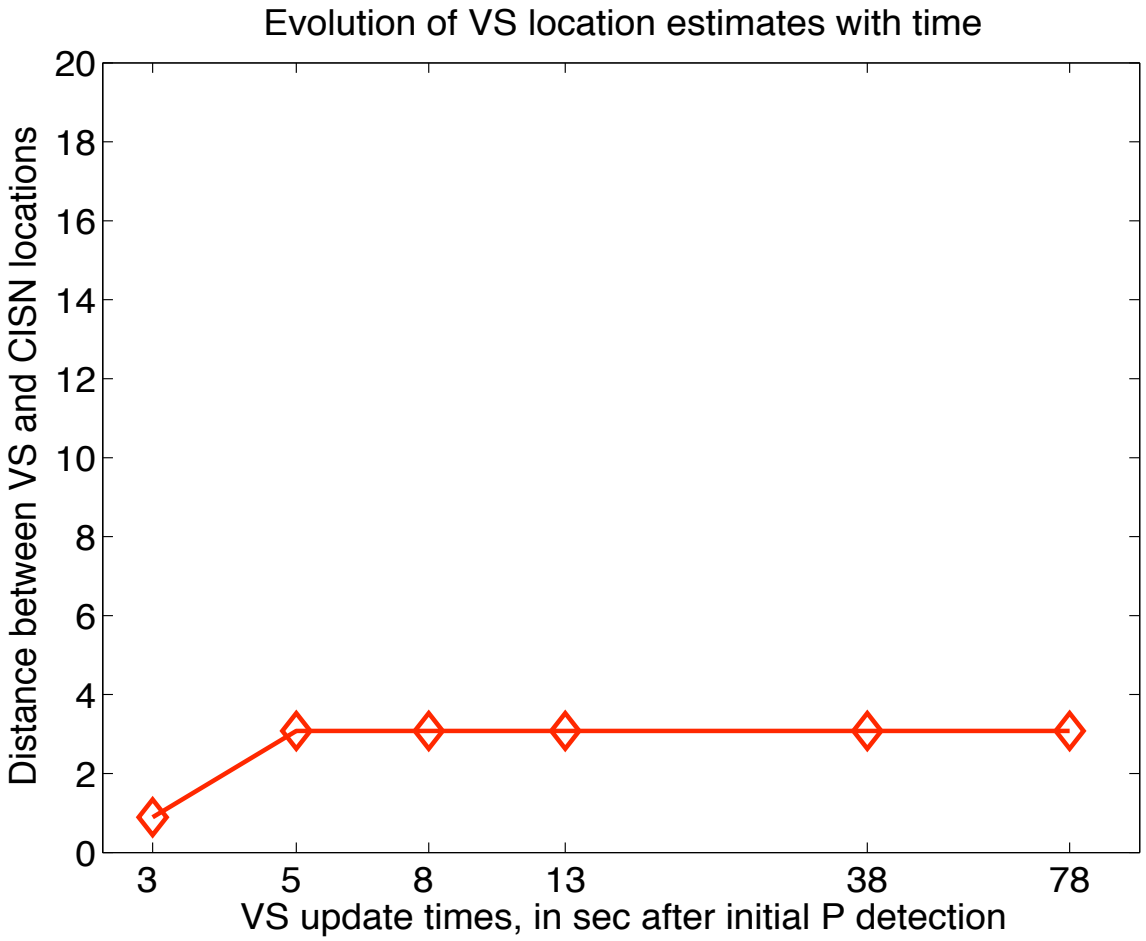

Figure 8.12: Plotted is the distance between the VS location estimate and the SCSN-reported location as a function of time. The VS location estimates do not change much with time, since the epicenter is uniquely determined by the P wave arrivals available at the time of the initial VS estimates. The VS locations are consistently within 4 km of the SCSN-reported epicenter.

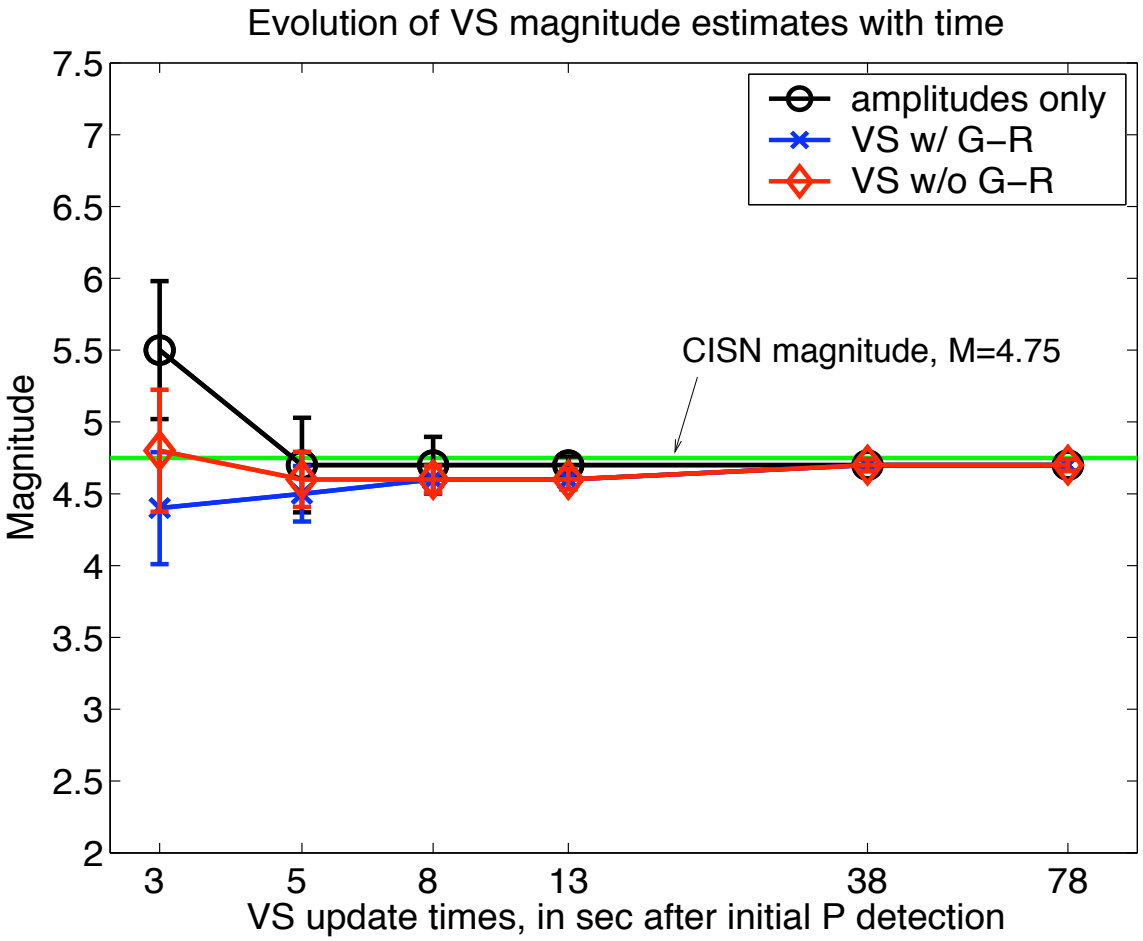

Figure 8.13: The evolution of various magnitude estimates as a function of time. The estimates labeled "amplitude only" correspond to not using any prior information. The VS magnitude estimates with and without the Gutenberg-Richter magnitude-frequency relationship in the Bayes prior are shown. The horizontal line denotes the SCSN magnitude of M=4.75. The VS estimate without G-R is within 0.05 magnitude units of the true magnitude at 3 seconds after the initial P detection.

initial P detection. The amplitude-based location (green contours) is obtained by finding the point source that best fits the distribution of peak P and S wave amplitudes from 89 stations at 80 seconds after the origin time. Since there is a general agreement between the amplitude- and arrival-based locations (they are within about 20 km of each other), the arrival-based location is correct.

Surprisingly, the magnitude estimates based on the vertical ground motion ratio, $Zad = acc^{0.37}/disp^{0.93}$ appear to have a relatively strong distance dependence. Ratio-based magnitude estimates from stations within 20 km of the epicenter are consistently larger than the actual magnitude of M=4.75. In contrast, the ratio-based magnitude estimates from the M=7.1 Hector Mine,M=6.5 San Simeon, and M=6.0 Parkfield earthquakes did not show this distance dependence. However, there were no stations within 20 km epicentral distance for these events. Whether or not the vertical ground motion ratios from stations relatively in-close characteristically overestimate magnitude is difficult to resolve. The dataset from which the ground motion ratio relationships were derived did not have much data at close distances. It is possible that the ground motion ratio magnitude estimators work best for stations at intermediate range distances ($>$ 20 km) away from the earthquake. This is not necessarily a problem; from geometric considerations, stations record more ground motions from events located more than about 20 km away than from events located within 20 km.

The observed peak vertical P-wave and rms horizontal S-wave amplitudes from the Yorba Linda mainshock as a function of epicentral distance are compared with the expected ground motion levels from an M=4.75 event as given by the envelope attenuation relationships in Chapter 2. (See Figures 8.16 and 8.17). There is a relatively good agreement between the observed and expected ground motion levels. This is what we would expect, since the Yorba Linda dataset was used to develop the said envelope attenuation relationships.

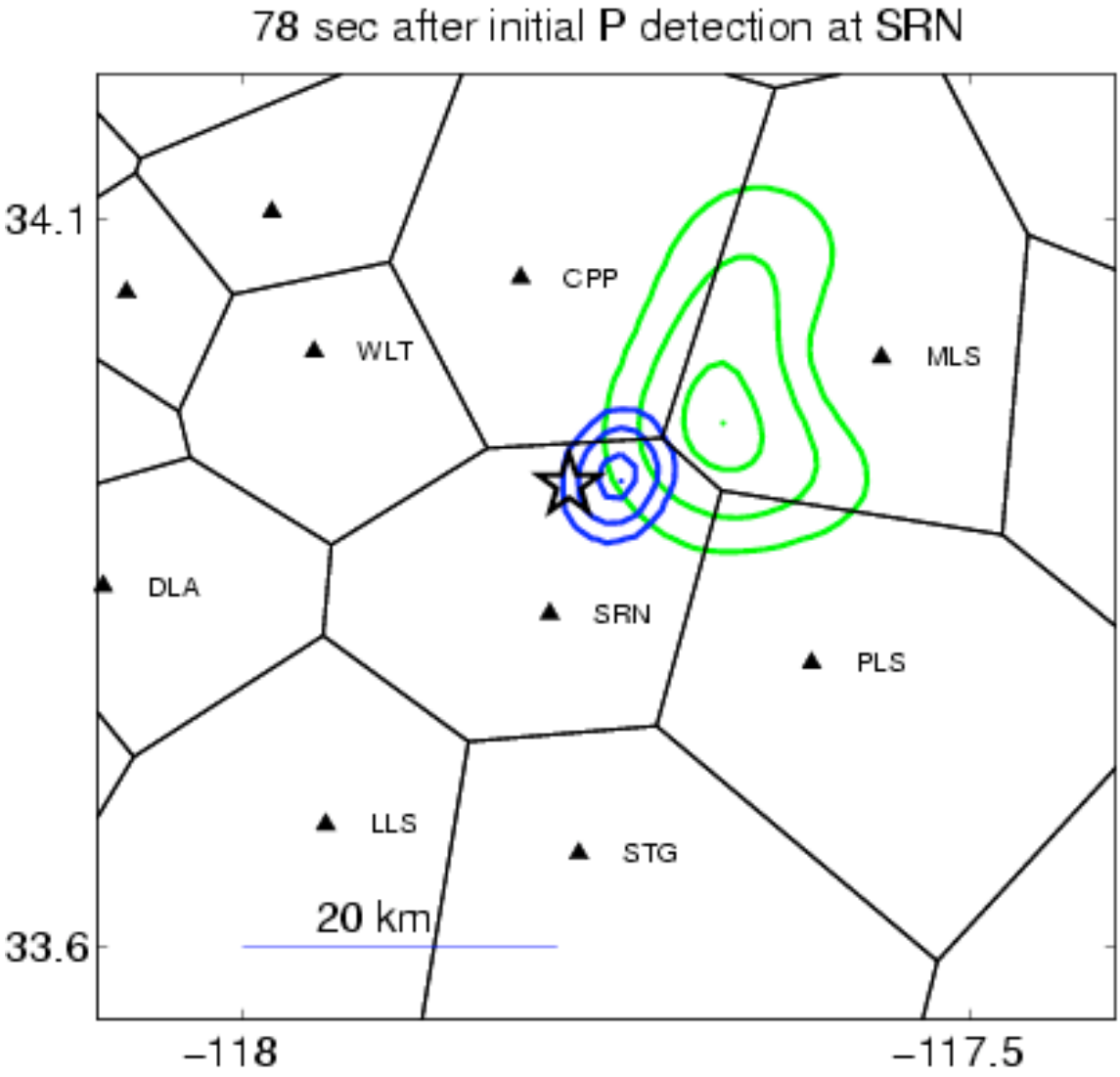

Figure 8.14: Comparison of amplitude- and arrival-based location estimates 78 seconds after the initial P detection (80 seconds after origin time). The amplitude-based location (green contours) is derived from the distribution of peak P- and S-wave amplitudes from 89 stations. The arrival-based location is obtained from 89 P arrivals. The arrival-based location in this analysis should match the SCSN-reported location, marked by a star. In general, the amplitude-based location is consistent with the arrival-based location (their contours overlap). Recall that these 2 different location estimates are relatively independent, since they were obtained from different sets of observations.

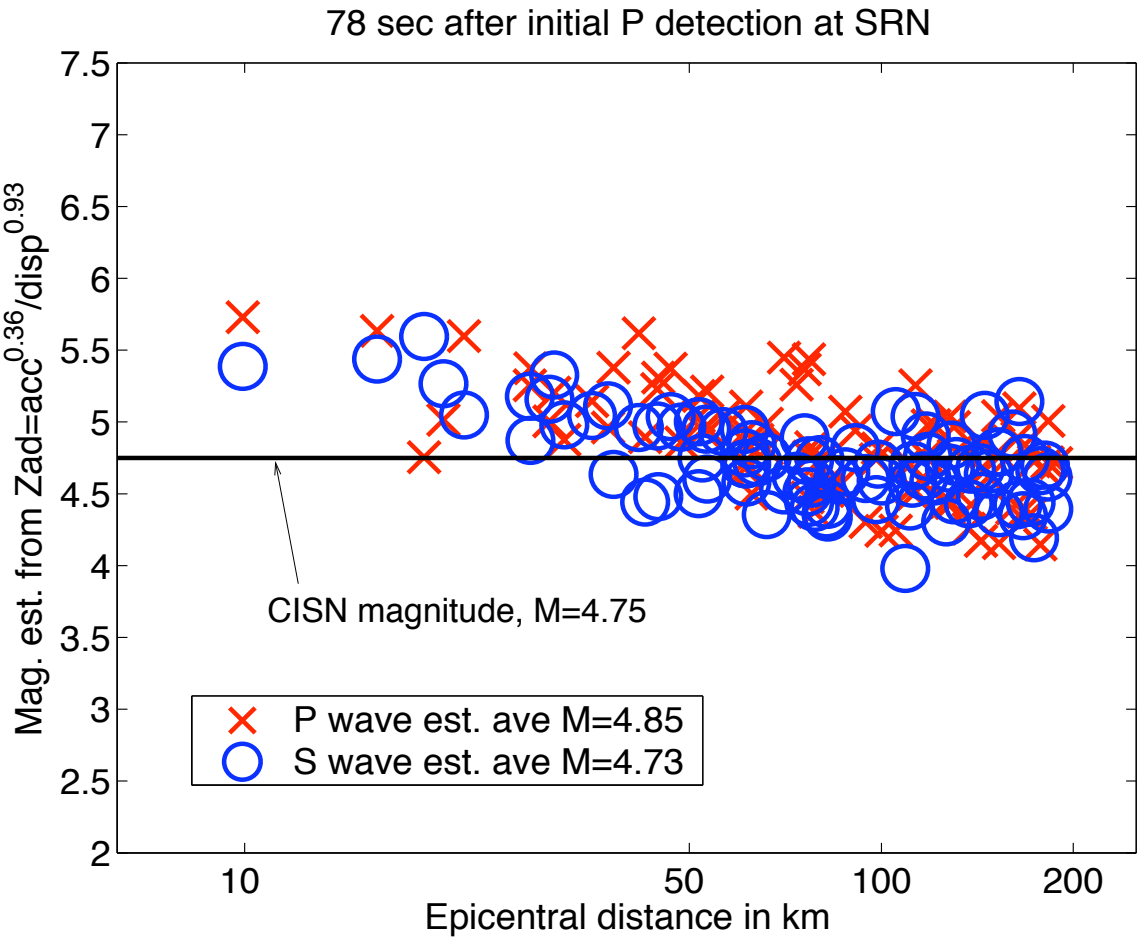

Figure 8.15: Magnitude estimates based on the vertical ground motion ratio, $Zad = acc^{0.36}/disp^{0.93}$, for P- and S-waves as a function of epicentral distance. It appears that the ratio-based magnitude estimates from stations within about 20 km epicentral distance are consistently larger than the actual magnitude of M=4.75. In contrast, the ratio-based magnitude estimates from the M=7.1 Hector Mine, M=6.5 San Simeon, and the M=6.0 Parkfield events show no distance-dependence.

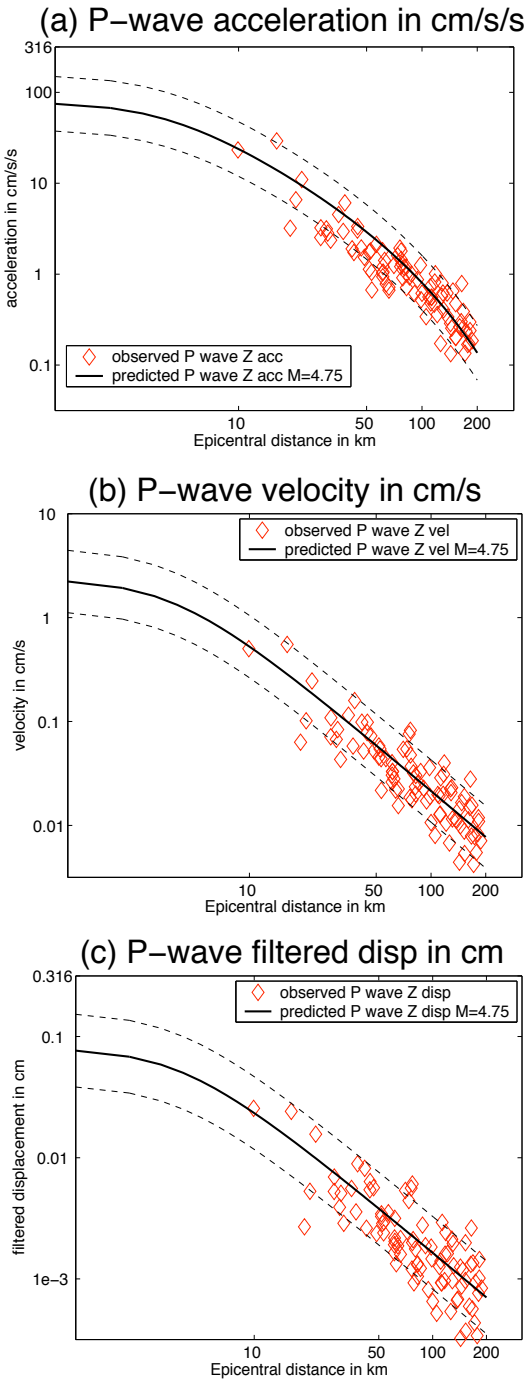

Figure 8.16: The predicted ground motion levels as a function of epicentral distance given by the vertical P-wave envelope attenuation relationships discussed in Chapter 2 for an M=4.75 event and the observed peak vertical (a) acceleration, (b) velocity, and (c) filtered displacement amplitudes from the M=4.75 Yorba Linda mainshock.

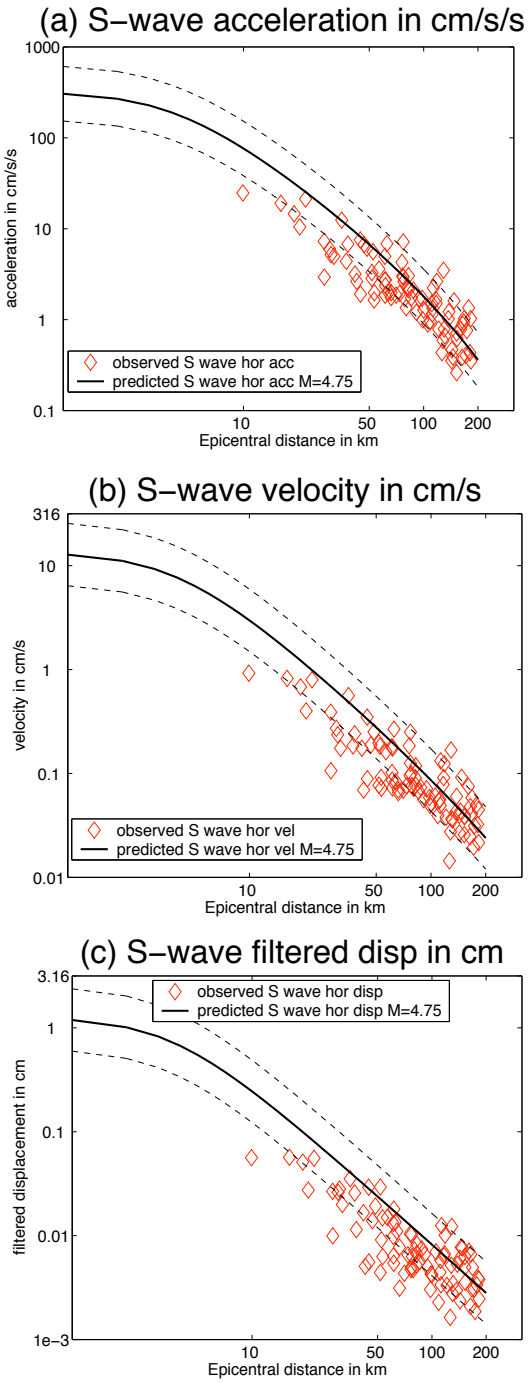

Figure 8.17: The predicted ground motion levels as a function of epicentral distance given by the rms horizontal S-wave envelope attenuation relationships discussed in Chapter2 for an M=4.75 earthquake and the observed peak rms horizontal S-wave (a) acceleration, (b) velocity, and (c) filtered displacement amplitudes from the M=4.75 Yorba Linda mainshock. The observed S-wave amplitudes seem to exhibit stronger saturation than would be expected from the envelope attenuation relationships. This may be due to the difficulty in distinguishing between P and S waves at close distances.